



Total Block Error Rate in Two-Way Semi-Duplex Relays with High SNR under Unknown Channel State Information

H. Hisarboni¹, Z. Keshavarz Gandomani^{1,*}

¹ Department of Telecommunications, Faculty of Electrical and Computer Engineering, Semnan University, Semnan, Iran

| ARTICLE INFO | ABSTRACT |
|--|---|
| <p>Article History: Received 10 May 2019 Received in revised form 14 June 2019 Accepted 15 September 2019 Available online 17 September 2019</p> | <p>In the fifth generation (5G) of telecommunications, two fundamental parameters—reliability and latency—are given special attention due to their critical role in supporting ultra-reliable and low-latency communications (URLLC). These parameters are essential for applications such as autonomous vehicles, remote surgery, and industrial automation, where even minimal delays or errors can have significant consequences. To meet the stringent demands of 5G systems, fundamental modifications in network architecture and transmission protocols are required. One such approach is reducing the length of transmitted packets to enhance efficiency while maintaining reliability. Cooperative relay networks play a key role in improving communication performance by enhancing signal strength and coverage. These networks are typically designed under the assumption that channel state information (CSI) is available at network nodes. However, in real-world scenarios, acquiring perfect CSI is challenging due to factors such as feedback delays, estimation errors, and hardware limitations. This study investigates a two-way semi-duplex relay system under conditions of small packet lengths and incomplete CSI, a situation that closely reflects practical 5G network constraints. In this paper, we derive an approximate analytical expression for the total block error rate (BLER) at high signal-to-noise ratios (SNR), which serves as a crucial performance metric for evaluating system reliability. Additionally, Monte Carlo simulations are performed to validate the accuracy of the analytical findings. The results demonstrate the impact of small packet lengths and imperfect CSI on system performance, providing valuable insights into the design of reliable 5G relay networks.</p> |
| <p>Keywords: Incomplete Channel State Information, Small Packets, Two-Way Semi-Duplex Relays, Block Error Rate</p> | |

1. INTRODUCTION

The fifth generation of telecommunications technology (5G) has made significant strides in enhancing data transmission quality and speed in wireless networks. This advanced technology revolutionizes communications across various fields, from smart vehicles and electronic devices to healthcare and education, ushering in a new era of connectivity [1-3]. A crucial function proposed for 5G networks is mission-critical communications, where reliability and latency are paramount [4, 5]. A prime example is remote surgery, where any connection drop or

* Corresponding Author: zahra_keshavarz@semnan.ac.ir

Department of Telecommunications, Faculty of Electrical and Computer Engineering, Semnan University, Semnan, Iran



excessive delay can endanger a patient's life. Another significant area where 5G can have a substantial impact is the Internet of Things (IoT) [2, 6]. IoT involves devices interconnected via the internet, capable of communicating with users, software, and other devices. Any device with a sensor for information exchange can be an IoT object, such as temperature sensors, traffic sensors, and energy measurement sensors [2, 7]. Data exchanged in IoT systems are often minimal, typically only a few bytes, making the use of large packets inefficient. Thus, to meet the upcoming demands of 5G communications, employing new methods and making fundamental changes in the structure of transmitted packets is essential [8, 9]. According to Shannon's theory, achieving the channel capacity rate is feasible with infinitely long packets, and sending and decoding relatively large packets introduces delay. Therefore, using limited and small-length packets for data transmission is highly efficient and attractive [8, 9].

Cooperative networks are also a promising solution for achieving high reliability and reducing transmission power compared to direct transmission in future wireless communication systems [10, 11]. Studies have shown that relays, as a primary cooperative technique, have significant potential in extending the communication range of wireless networks. Two-way relays, which have double the spectral efficiency of one-way relays, have garnered substantial research interest [2-6]. To fully harness the potential of two-way relays, accurate and complete estimation of channel state information (CSI) is essential, and one method to obtain CSI is through channel estimation techniques [12, 13]. However, nearly all existing works on two-way relays assume complete CSI availability, with relatively little attention given to the impact of incomplete CSI estimation. Hence, this paper focuses on two-way relays with imperfect CSI estimation, considering small packet lengths, and assumes that information exchange between two source nodes occurs over two time slots. In the first time slot, both source nodes simultaneously send information to the relay node. In the second time slot, the relay processes the received information and forwards it back to the two source nodes using one of the cooperative transmission methods such as decode-and-forward (DF), amplify-and-forward (AF), or compress-and-forward (CF).

Reliability can be defined as the probability of successful data bit transmission within a specific time and under particular channel conditions. Therefore, to maximize the reliability of transmitting each packet (block), the error rate must be minimized. The block error rate is the probability of error in the blocks transmitted from the sender to the receiver. This paper considers the block error rate as a metric for evaluation. Studies on the performance of cooperative relay networks with small packet lengths can be broadly categorized into two groups: the first group of references assumes complete CSI at the nodes for system performance analysis [14-18]. For instance, in [18], researchers derived the block error rate expression for one-way and full-duplex two-way relays and compared the performance of these two systems. Reference [16] examined two schemes for two-way relays with three time slots and two time slots (two-way semi-duplex relays) and derived an approximate expression for the total block error rate at high SNR for these systems, comparing the two schemes. The relay used in these schemes was of the semi-duplex type. The second group of studies, which are more realistic, examines the impact of estimation errors on system performance [19-21]. For example, in [19], the author proposed a power allocation problem to maximize the throughput of a one-way relay, assuming CSI is not available at the source.

To date, researchers have not investigated the total block error rate of two-way semi-duplex relays at high SNR, assuming incomplete CSI at the nodes and considering small packet lengths. This motivates the present study. The system model is described in Section 2. In Section 3, the total block error rate for two-way semi-duplex relays at high SNR is derived. Simulation results are presented in Section 4, followed by conclusions in Section 5.

2. SYSTEM MODEL

Consider a two-way semi-duplex relay system as shown in Figure 1, assuming that channel information is not available at either the nodes or the relay, and there is no direct path between the two nodes. The channel coefficient between node A and the relay is denoted by h , and the channel coefficient between node B and the relay is denoted by g , with the channels following a Rayleigh fading model. It is also assumed that the channel coefficients remain constant over two consecutive time slots: from the nodes to the relay and from the relay to the nodes.

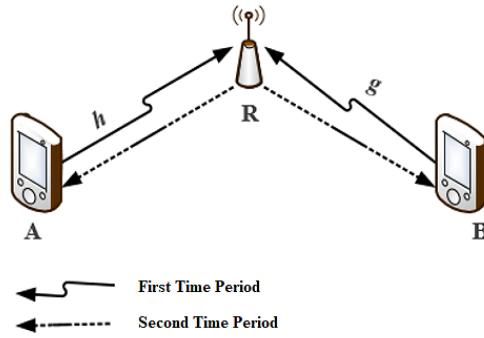


Fig.1. Two-way semi-duplex relay

In this scenario, two nodes, A and B, intend to send small packets via relay R in two consecutive time slots. In the first time slot, nodes A and B simultaneously transmit small packets S_A and S_B of lengths m_A and m_B symbols, respectively, to relay R with powers P_A and P_B . In the second time slot, relay R processes and amplifies the received signal, subject to power constraints, and retransmits it to both nodes A and B with power P_R . Upon receiving the relayed packet, each node A and B, leveraging prior knowledge of their own transmitted packet, cancels the effect of their own transmission from the received signal. Consequently, the packet sent by node A will be received and decoded by node B, and vice versa. For simplicity, we assume the packet lengths are equal, i.e., $m_A=m_B=m_H$. Given that the transmission of a packet of length m_H symbols between two nodes requires $m=2m_H$ channel uses (m_H uses in the first time slot and m_H uses in the second time slot), the packet length is expressed in terms of each channel use as mm . Based on the provided explanations, the signal received at relay R can be expressed as follows:

$$y_R = \sqrt{P_A} h S_A + \sqrt{P_B} g S_B + w_R \tag{1}$$

Additionally, the relay receiver is subject to additive white Gaussian noise (AWGN) with zero mean and variance N_0 . The retransmitted signal, after being amplified by the relay, is expressed as follows

$$S_R = G y_R^* \tag{2}$$

where $(.)^*$ denotes the complex conjugate of G is the relay amplification gain, which is variable. An amplify-and-forward (AF) relay with variable gain requires real-time channel state information at the relay. Thus, G varies according to the channel conditions, but the relay's transmit power remains constant under different channel conditions. Therefore, G can be expressed as:

$$G = \sqrt{\frac{P_R}{P_A |h|^2 + P_B |g|^2 + N_0}} \tag{3}$$

The received packets at nodes A and B can be written as:

$$y_A = G \sqrt{P_B} h g^* S_B^* + G \sqrt{P_A} |h|^2 S_A^* + G h w_R^* + w_A \tag{4}$$

$$y_B = G \sqrt{P_A} g h^* S_A^* + G \sqrt{P_B} |g|^2 S_B^* + G g w_R^* + w_B \tag{5}$$

Where w_A and w_B are additive white Gaussian noise (AWGN) components with zero mean and variance N_0 , respectively. As mentioned, nodes A and B, being aware of their own transmitted packet information, subtract the effect of their own packets from the relay-received packets. Therefore, the second terms in equations (4) and (5) can be eliminated. Consequently, the received packets can be rewritten as:

$$y_A = G \sqrt{P_B} h g^* S_B^* + G h w_R^* + w_A \tag{6}$$

$$y_B = G\sqrt{P_A}gh^*S_A^* + Ggw_R^* + w_B \tag{7}$$

The channel coefficients are modeled as:

$$h = \tilde{h} + \lambda_{eh} \tag{8}$$

$$g = \tilde{g} + \lambda_{eg}$$

where \tilde{h} and \tilde{g} are the estimated channel coefficients from node A to the relay and from node B to the relay, respectively. λ_{eh} and λ_{eg} are the channel estimation errors. It is assumed that the channel estimation errors have zero mean and variances σ_{eh}^2 and σ_{eg}^2 . For simplicity, orthogonality between the channel coefficient estimates and the error components is assumed. Therefore, the second moment of each channel coefficient can be expressed as:

$$\mathbb{E}\left[|h|^2\right] = \mathbb{E}\left[\left(\tilde{h} + \lambda_{eh}\right)\left(\tilde{h} + \lambda_{eh}\right)^*\right] = |\tilde{h}|^2 + \sigma_{eh}^2 \tag{9}$$

$$\mathbb{E}\left[|g|^2\right] = \mathbb{E}\left[\left(\tilde{g} + \lambda_{eg}\right)\left(\tilde{g} + \lambda_{eg}\right)^*\right] = |\tilde{g}|^2 + \sigma_{eg}^2$$

Since nodes A and B are mathematically symmetrical, we will focus on the packet received by node B. By substituting the channel coefficient estimation error into equation (7), we can rewrite it as follows:

$$y_B = G\sqrt{P_A}\tilde{g}\tilde{h}^*S_A^* + \lambda_B + w_N \tag{10}$$

In equation (10), the values of λ_B and w_N are equivalent to:

$$\lambda_B = G\sqrt{P_A}\tilde{g}\lambda_{eh}^*S_A^* + G\sqrt{P_A}\tilde{h}^*\lambda_{eg}S_A^* + G\sqrt{P_A}\lambda_{eg}\lambda_{eh}^*S_A^* \tag{11}$$

$$w_N = G\tilde{g}w_R^* + G\lambda_{eg}w_R^* + w_B$$

Additionally, the relay gain factor, considering the estimation error of the channel coefficients, can be rewritten as:

$$\tilde{G} = \sqrt{\frac{P_R}{P_A|\tilde{h}|^2 + P_B|\tilde{g}|^2 + P_A\sigma_{eh}^2 + P_B\sigma_{eg}^2 + N_0}} \tag{12}$$

Finally, by substituting equation (12) into equation (10), we can derive the signal-to-noise power ratio for node B as:

$$\gamma_B = P_R P_A \frac{|\tilde{h}|^2 |\tilde{g}|^2}{\left\{ \left(P_R P_A \sigma_{eh}^2 + P_R N_0 + P_B N_0 \right) |\tilde{g}|^2 \right.}$$

$$+ \left. \left(P_R P_A \sigma_{eg}^2 + P_A N_0 \right) |\tilde{h}|^2 + P_R P_A \sigma_{eg}^2 \sigma_{eh}^2 + P_R \sigma_{eg}^2 N_0 \right.}$$

$$\left. + P_A \sigma_{eh}^2 N_0 + P_B \sigma_{eg}^2 N_0 + N_0^2 \right\}$$

$$\tag{13}$$

3. SUM OF THE BLOCK ERROR RATE FOR TWO-WAY SEMI-DUPLEX RELAYS

In this section, we approximately derive the sum of the block error rate for two-way semi-duplex relays at high SNR values. Assume that k bits at the transmitter are encoded into m_H symbols, and these symbols are sent as a packet or block of m_H symbols to the receiver. Therefore, the transmission rate is defined as [2,16]:

$$r_H = \frac{k}{m_H} \tag{14}$$

The sum of the block error rate for two-way semi-duplex relays can be expressed as:

$$\mathcal{E}_H = \Psi_{H_A} + (1 - \Psi_{H_A}) \Psi_{H_B} \approx \Psi_{H_A} + \Psi_{H_B} \tag{15}$$

In the above equation, Ψ_{H_A} and Ψ_{H_B} represent the block error rates for the channels from node A to relay R and from node B to relay R, respectively. Generally, $\Psi_{H_\tau} (\tau \in \{A, B\})$ is calculated [22,23] as:

$$\Psi_{H_\tau} = \mathbb{E} \left[Q \left(\frac{C(\gamma_{H_\tau}) - r_H}{\sqrt{V(\gamma_{H_\tau})/m_H}} \right) \right] \tag{16}$$

Considering that equation (16) involves the Q-function, which has its inherent complexity, we use the equivalent linear approximation given in Equation (17) [18,16]:

$$Q \left(\frac{C(\gamma_{H_\tau}) - r_H}{\sqrt{V(\gamma_{H_\tau})/m_H}} \right) \approx \Xi(x) \tag{17}$$

$$\Xi(x) = \begin{cases} 1 & \gamma_{H_\tau} \leq \zeta_H \\ \frac{1}{2} - \mathcal{G}_H \sqrt{m_H} (\gamma_{H_\tau} - \theta_H) & \zeta_H < \gamma_{H_\tau} < \xi_H \\ 0 & \gamma_{H_\tau} \geq \xi_H \end{cases}$$

Each parameter used in equation (17) is equivalent to:

$$\mathcal{G}_H = \frac{1}{2\pi\sqrt{2^{2r_H} - 1}} \tag{18}$$

$$\theta_H = 2^{r_H} - 1$$

$$\xi_H = \theta_H + \frac{1}{2\mathcal{G}_H\sqrt{m_H}}$$

$$\zeta_H = \theta_H - \frac{1}{2\mathcal{G}_H\sqrt{m_H}}$$

Based on equation (17), equation (16) can be rewritten as follows [16,18]:

$$\Psi_{H_\tau} = \int_0^\infty Q \left(\frac{C(\gamma_{H_\tau}) - r_H}{\sqrt{V(\gamma_{H_\tau})/m_H}} \right) f_{\gamma_{H_\tau}}(x) dx \tag{19}$$

$$\approx \int_0^\infty \Xi(x) f_{\gamma_{H_\tau}}(x) dx \approx \int_0^\infty \Xi(x) dF_{\gamma_{H_\tau}}(x)$$

$$= \left[\Xi(x) F_{\gamma_{H_\tau}}(x) \right]_0^\infty - \int_0^\infty F_{\gamma_{H_\tau}}(x) d\Xi(x)$$

$$= \mathcal{G}_H \sqrt{m_H} \int_{\zeta_H}^{\xi_H} F_{\gamma_{H_\tau}}(x) dx$$

Here, $f_{\gamma_{H_\tau}}(\cdot)$ and $F_{\gamma_{H_\tau}}(\cdot)$ represent the probability density function and the cumulative distribution function of the variable $\gamma_{H_\tau} (\tau \in \{A, B\})$, respectively. $F_{\gamma_{H_\tau}}(\gamma_{th})$ is given by [12]:

$$F_{\gamma_{H_\tau}}(\gamma_{th}) = P_{out_\tau}(\gamma_{H_\tau} < \gamma_{th}) = 1 - z_\tau \exp(-a_\tau) K_1(z_\tau) \tag{20}$$

In equation (20), γ_{th} is the SNR threshold value, and $K_1(\cdot)$ is the modified Bessel function of the second kind of order one [24]. The equivalent parameters z_τ and a_τ for nodes A and B are specified in Table 1.

Table 1. Required Parameters for Nodes A and B

| Variable | B | A |
|----------|--|--|
| a | $\frac{(\mu_h \alpha_B + \mu_g \beta_B) \gamma_{th}}{P_R P_A}$ | $\frac{(\mu_g \alpha_A + \mu_h \beta_A) \gamma_{th}}{P_R P_B}$ |
| z | $\sqrt{\frac{4\mu_h \mu_g (\gamma_{th}^2 \alpha_B \beta_B + \gamma_{th} \delta_B P_R P_A)}{P_A^2 P_R^2}}$ | $\sqrt{\frac{4\mu_h \mu_g (\gamma_{th}^2 \alpha_A \beta_A + \gamma_{th} \delta_A P_R P_B)}{P_B^2 P_R^2}}$ |
| α | $P_R P_A \sigma_{eh}^2 + P_R N_0 + P_B N_0$ | $P_R P_B \sigma_{eg}^2 + P_R N_0 + P_A N_0$ |
| β | $P_R P_A \sigma_{eg}^2 + P_A N_0$ | $P_R P_B \sigma_{eh}^2 + P_B N_0$ |
| δ | $P_R P_A \sigma_{eg}^2 \sigma_{eh}^2 + P_R \sigma_{eg}^2 N_0$ $+ P_A \sigma_{eh}^2 N_0 + P_B \sigma_{eg}^2 N_0 + N_0^2$ | $P_R P_B \sigma_{eg}^2 \sigma_{eh}^2 + P_R \sigma_{eh}^2 N_0$ $+ P_B \sigma_{eg}^2 N_0 + P_A \sigma_{eh}^2 N_0 + N_0^2$ |

In Table 1, the values of μ_h and μ_g are defined as:

$$\mu_h = \frac{1}{\mathbb{E}[|h|^2] - \sigma_{eh}^2} = \frac{1}{\sigma_h^2 - \sigma_{eh}^2} \tag{21}$$

$$\mu_g = \frac{1}{\mathbb{E}[|g|^2] - \sigma_{eg}^2} = \frac{1}{\sigma_g^2 - \sigma_{eg}^2}$$

The lower bound of the average symbol error rate can be written as: $F_{\gamma_{H_\tau}}(\gamma_{th})$

$$F_{\gamma_{H_\tau}}(\gamma_{th}) \geq F_{\gamma_{H_\tau}}^{lb} = 1 - \exp(-a_\tau) \tag{22}$$

By considering the relationship in (22) and its Taylor series expansion, the lower bound of the average symbol error rate can be approximated as:

$$F_{\gamma_{H_\tau}}^{lb} = a_\tau \tag{23}$$

Furthermore, using the relationships in (19) and (23), the value of Ψ_{H_B} can be computed as:

$$\begin{aligned}
 \Psi_{H_B}^{\infty} &= \mathcal{G}_H \sqrt{m_H} \int_{\zeta_H}^{\xi_H} F_{\gamma_{H_B}}^{lb}(x) dx & (24) \\
 &= \mathcal{G}_H \sqrt{m_H} \int_{\zeta_H}^{\xi_H} a_B dx \\
 &= \mathcal{G}_H \sqrt{m_H} \int_{\zeta_H}^{\xi_H} \frac{(\mu_h \alpha_B + \mu_g \beta_B)x}{P_R P_A} dx \\
 &= \frac{\mathcal{G}_H \sqrt{m_H} (\mu_h \alpha_B + \mu_g \beta_B)}{2 P_R P_A} x^2 \Big|_{\zeta_H}^{\xi_H} \\
 &= \frac{\mathcal{G}_H \sqrt{m_H} (\mu_h \alpha_B + \mu_g \beta_B)}{2 P_R P_A} \left(4\theta_H \frac{1}{2\mathcal{G}_H \sqrt{m_H}} \right) = \frac{(\mu_h \alpha_B + \mu_g \beta_B)}{P_R P_A} \theta_H
 \end{aligned}$$

Similarly, the value of Ψ_{H_A} can be obtained for high SNR values. Finally, the total block error rate of the dual-hop, half-duplex relay system, considering the channel coefficient estimation error, can be expressed as:

$$\mathcal{E}_H^{\infty} \approx \Psi_{H_A}^{\infty} + \Psi_{H_B}^{\infty} = \left(\frac{(\mu_h \alpha_B + \mu_g \beta_B)}{P_R P_A} + \frac{(\mu_g \alpha_A + \mu_h \beta_A)}{P_R P_B} \right) \theta_H \tag{25}$$

4. SIMULATION AND RESULTS PRESENTATION

In this section, we present the simulation and results. Our theoretical results are validated through Monte Carlo simulations, with each simulation run generating a number of samples. In the plotted graphs, the relay's position is exactly in the middle of nodes A and B, normalized such that $d_A + d_B = 1$. The distance from the relay to node A is d_A and to node B is d_B . The path loss exponent in these figures is denoted as $\beta = 4$. Additionally, in these figures, the number of transmitted bits, $k = 100$ is considered.

In Figure 2, the total block error rate of two-way half-duplex relays is plotted against different values of P_A . In this figure, the transmission power of node A and the transmission power of node R are assumed to be equal, ($P_A = P_R$). The total block error rate of two-way half-duplex relays is compared for the cases when channel state information (CSI) is available and when it is not. It is worth noting that the total block error rate of two-way half-duplex relays with available CSI has been examined in reference [16]. According to the figure, it can be observed that when the channel estimation error is high ($\sigma_{eh}^2 = \sigma_{eg}^2 = 0.1$), the total block error rate of two-way half-duplex relays also increases. Furthermore, as the SNR increases, the difference between the total block error rate curves for cases with and without available CSI increases. This is because, at high SNR values, the total block error rate of two-way half-duplex relays decreases when CSI is available, while for the case without CSI, the curve enters a region known as the error floor. The error floor region is characterized by high SNR where the probability of channel failure is low, and unexpectedly, the slope of the curve suddenly decreases and remains within a specific error range. On the other hand, given that in the derived relationships for the total block error rate, the lower bound of the cumulative distribution function (CDF) of the variable γ_{H_τ} was approximated, this approximation causes the Monte Carlo simulation results to lie above our approximate results.

In Figure 3, the total block error rate of two-way half-duplex relays is plotted against different block lengths. According to Figure 3, it can also be stated that the larger the block length, the lower the total block error rate of the system model, as longer block lengths allow for the design of stronger error correction and detection codes. Additionally, this figure shows that due to the approximation of the lower bound of the CDF of the variable γ_{H_τ} , the Monte Carlo simulation results are above our approximate results.

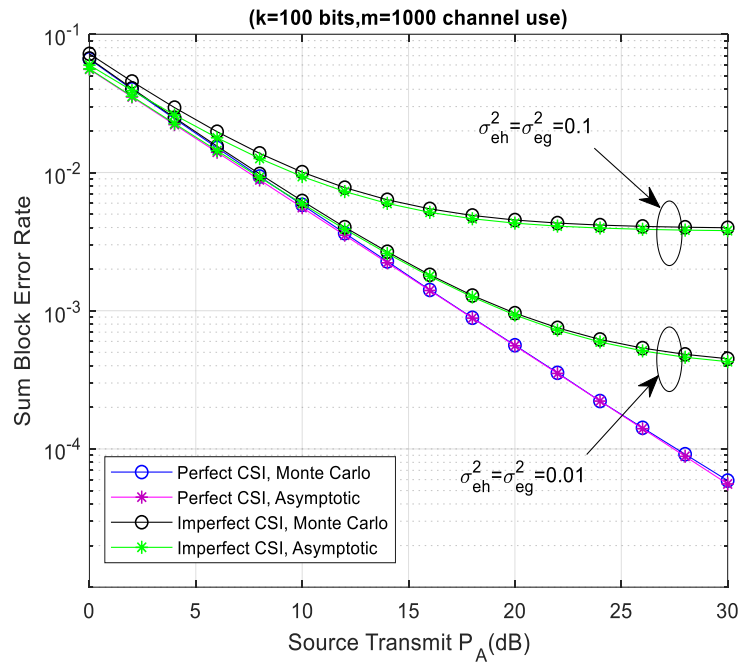


Fig.2. Total Block Error Rate of Two-Way Semi-Relay Blocks Based on Different P_A

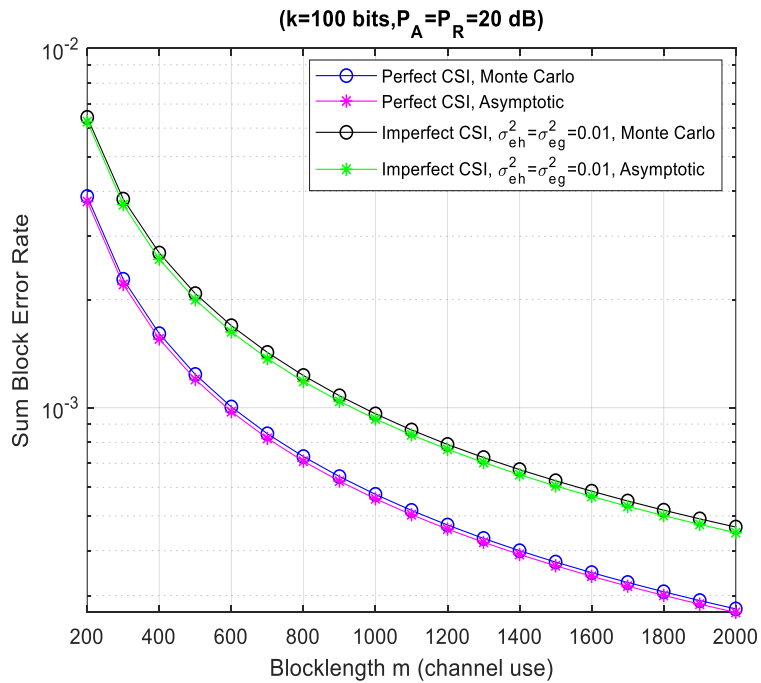


Fig.3. Total Block Error Rate of Two-Way Semi-Relay Blocks Versus Different Block Lengths m

5. CONCLUSION

In this paper, we examined two-way semi-relay systems under scenarios involving packets with small lengths, and we investigated the impact of channel estimation errors as incomplete information on the channel conditions on the performance of the two-way semi-relay system. Among various network performance evaluation criteria, we focused on the block error rate and derived an approximate expression for the total block error rate of two-way semi-relay systems at high SNR values. By conducting Monte Carlo simulations, we validated the accuracy of the analytical results obtained. The simulation results indicated that as the length of the transmitted packets (blocks) increases, the total block error rate of the system model decreases. This is because, under these conditions, stronger error correction and error detection codes can be designed. Furthermore, the results showed that when the error in channel coefficient estimation is high, the total block error rate of the two-way semi-relay systems also increases.

Transparency Statement

The data supporting this study are available upon reasonable request to the corresponding author, subject to ethical and confidentiality considerations.

Acknowledgments

We would like to express our gratitude to all individuals who contributed to this project.

Declaration of Interest

The authors declare that they have no competing interests.

Funding

This research received no specific grant from any funding agency, commercial, or not-for-profit sectors.

REFERENCES

- [1] G. J. Sutton et al. (2019). Enabling Technologies for Ultra-Reliable and Low Latency Communications: From PHY and MAC Layer Perspectives. *IEEE Communications Surveys & Tutorials*. <https://doi.org/10.1109/COMST.2019.2897800>
- [2] G. Durisi, T. Koch, & P. Popovski. (2016). Toward massive, ultrareliable, and low-latency wireless communication with short packets. *Proceedings of the IEEE*, 104(9), 1711-1726. <https://doi.org/10.1109/JPROC.2016.2537298>
- [3] P. Yang, Y. Xiao, M. Xiao, & S. Li. (2019). 6G Wireless Communications: Vision and Potential Techniques. *IEEE Network*, 33(4), 70-75. <https://doi.org/10.1109/MNET.2019.1800418>
- [4] D. Qiao, M. C. Gursoy, & S. Velipasalar. (2019). Throughput-Delay Tradeoffs with Finite Blocklength Coding over Multiple Coherence Blocks. *IEEE Transactions on Communications*. <https://doi.org/10.1109/TCOMM.2019.2919637>
- [5] M. Shirvanimoghaddam et al. (2018). Short block-length codes for ultra-reliable low latency communications. *IEEE Communications Magazine*, 57(2), 130-137. <https://doi.org/10.1109/MCOM.2018.1800181>

- [6] Y. Hu, Y. Zhu, M. C. Gursoy, & A. Schmeink. (2018). SWIPT-enabled relaying in IoT networks operating with finite blocklength codes. *IEEE Journal on Selected Areas in Communications*, 37(1), 74-88. <https://doi.org/10.1109/JSAC.2018.2872361>
- [7] C. She, C. Yang, & T. Q. Quek. (2017). Radio resource management for ultra-reliable and low-latency communications. *IEEE Communications Magazine*, 55(6), 72-78. <https://doi.org/10.1109/MCOM.2017.1601092>
- [8] M. Shirvanimoghaddam et al. (2019). Short Block-Length Codes for Ultra-Reliable Low Latency Communications. *IEEE Communications Magazine*, 57(2), 130-137. <https://doi.org/10.1109/MCOM.2018.1800181>
- [9] B. Makki, T. Svensson, G. Caire, & M. Zorzi. (2019). Fast HARQ over Finite Blocklength Codes: A Technique for Low-Latency Reliable Communication. *IEEE Transactions on Wireless Communications*, 18(1), 194-209. <https://doi.org/10.1109/TWC.2018.2878713>
- [10] Y. Han, S. H. Ting, C. K. Ho, & W. H. Chin. (2009). Performance bounds for two-way amplify-and-forward relaying. *IEEE Transactions on Wireless Communications*, 8(1), 432-439. <https://doi.org/10.1109/TWC.2009.080316>
- [11] G. Liu, F. R. Yu, H. Ji, V. C. Leung, & X. Li. (2015). In-band full-duplex relaying: A survey, research issues and challenges. *IEEE Communications Surveys & Tutorials*, 17(2), 500-524. <https://doi.org/10.1109/COMST.2015.2394324>
- [12] S. Wang, M. Wang, B. Jia, & Y. Li. (2016). Outage analysis of two-way amplify-and-forward relaying system with imperfect channel state information. In *2016 2nd IEEE International Conference on Computer and Communications (ICCC)*, 1642-1646. IEEE.
- [13] D. Choi & J. H. Lee. (2014). Outage probability of two-way full-duplex relaying with imperfect channel state information. *IEEE Communications Letters*, 18(6), 933-936. <https://doi.org/10.1109/LCOMM.2014.2320940>
- [14] Y. Hu, J. Gross, & A. Schmeink. (2016). On the capacity of relaying with finite blocklength. *IEEE Transactions on Vehicular Technology*, 65(3), 1790-1794. <https://doi.org/10.1109/TVT.2015.2406952>
- [15] Y. Hu, J. Gross, & A. Schmeink. (2015). On the performance advantage of relaying under the finite blocklength regime. *IEEE Communications Letters*, 19(5), 779-782. <https://doi.org/10.1109/LCOMM.2015.2410770>
- [16] Y. Gu, H. Chen, Y. Li, L. Song, & B. Vucetic. (2018). Short-packet two-way amplify-and-forward relaying. *IEEE Signal Processing Letters*, 25(2), 263-267. <https://doi.org/10.1109/LSP.2017.2782828>
- [17] Y. Hu, C. Schnelling, Y. Amraue, & A. Schmeink. (2017). Finite blocklength performance of a multi-relay network with best single relay selection. In *2017 International Symposium on Wireless Communication Systems (ISWCS)*, 122-127. IEEE. <https://doi.org/10.1109/ISWCS.2017.8108095>
- [18] Y. Gu, H. Chen, Y. Li, & B. Vucetic. (2018). Ultra-reliable short-packet communications: Half-duplex or full-duplex relaying? *IEEE Wireless Communications Letters*, 7(3), 348-351. <https://doi.org/10.1109/LWC.2017.2777857>
- [19] Y. Hu, A. Schmeink, & J. Gross. (2018). Optimal scheduling of reliability-constrained relaying system under outdated CSI in the finite blocklength regime. *IEEE Transactions on Vehicular Technology*, 67(7), 6146-6155. <https://doi.org/10.1109/TVT.2018.2811943>
- [20] P. Nouri, H. Alves, R. D. Souza, & M. Latva-aho. (2019). In-Band Pilot Overhead in Ultra-Reliable Low

Latency Decode and Forward Relaying. In *2019 IEEE 89th Vehicular Technology Conference (VTC2019-Spring)*, 1-5. IEEE. <https://doi.org/10.1109/VTCSpring.2019.8746566>

- [21] O. L. A. López, E. M. G. Fernández, R. D. Souza, & H. Alves. (2018). Ultra-reliable cooperative short-packet communications with wireless energy transfer. *IEEE Sensors Journal*, 18(5), 2161-2177. <https://doi.org/10.1109/JSEN.2018.2789480>
- [22] W. Yang, G. Durisi, T. Koch, & Y. Polyanskiy. (2014). Quasi-static multiple-antenna fading channels at finite blocklength. *IEEE Transactions on Information Theory*, 60(7), 4232-4265. <https://doi.org/10.1109/TIT.2014.2318726>
- [23] Y. Polyanskiy, H. V. Poor, & S. Verdú. (2010). Channel coding rate in the finite blocklength regime. *IEEE Transactions on Information Theory*, 56(5), 2307. <https://doi.org/10.1109/TIT.2010.2043769>
- [24] A. Jeffrey & D. Zwillinger. (2007). *Table of integrals, series, and products*. Elsevier.